# RNA Folding: Thermodynamic and Molecular Descriptions of the Roles of Ions

David E. Draper
Department of Chemistry, The Johns Hopkins University, Baltimore, Maryland 21218

ABSTRACT The stability of a compact RNA tertiary structure is exquisitely sensitive to the concentrations and types of ions that are present. This review discusses the progress that has been made in developing a quantitative understanding of the thermodynamic parameters and molecular detail that underlie this sensitivity, including the nature of the ion atmosphere, the occurrence of specific ion binding sites, and the importance of the ensemble of partially unfolded states from which folding to the native structure occurs.

## INTRODUCTION

For ~20 years, the familiar ''L'' shape of transfer RNA was the only example of an RNA tertiary structure resolved at atomic resolution. Starting with the publication of the structure of a 160 nt domain of a self-splicing RNA a decade ago (1), many more surprisingly intricate and compact RNA structures, responsible for a variety of cellular functions, have been elucidated. An obvious energetic barrier to the formation of these structures is the high negative charge density that originates from the full negative charge of each backbone phosphate. Mobile ions would be expected to mitigate this electrostatic penalty, and in fact the sensitivity of RNA folding reactions to added salts was already apparent in early studies of tRNAs (2,3). The response of RNAs to ions is relevant to the assembly of some cellular machinery, such as ribosomes and spliceosomes, and also to the functional capabilities of many RNAs. Prime examples of the latter are so-called riboswitch RNAs, which adopt alternative folds in response to the concentrations of specific cellular metabolites (4). To understand how RNAs function in vivo, a quantitative understanding of the ways the ionic milieu of the cell may stabilize RNA structures is needed.

A useful framework for the equilibrium folding of RNA is the scheme

$$U \rightarrow I \rightarrow N.$$

Under fully denaturing conditions, the RNA lacks any hydrogen bonds between bases (the unfolded $U$ state), but secondary structures readily form in low concentrations of monovalent cations (an intermediate, or $I$ state). The native ($N$ state) functional conformation of many RNAs requires additional tertiary contacts, which are often stable only in the presence of divalent cations or a specific binding protein or ligand. This review focuses on the effects of ions on the $I \rightarrow N$ transition.

### Ion environments in and near RNA molecules

RNAs function in the intracellular ionic milieu, in which $K^+$ and $Mg^{2+}$ are the predominant cations. The thermodynamic activity of $K^+$ in *Escherichia coli* growing in standard media is estimated as ~0.11 M (5), equivalent to the mean ionic activity of an ~0.15 M KCl solution; more than fivefold higher activities can be reached in high osmolality media. The in vivo $Mg^{2+}$ activity is roughly equivalent to that of a solution containing 0.5–1.0 mM $Mg^{2+}$ and 0.15 M monovalent salt (6,7). Organic cations (such as spermidine or putrescine) are also present, though their effective concentrations have not been estimated and little work has been done on their effects on RNA folding.

In an instantaneous snapshot of an RNA in a cell, ions would be observed in a variety of environments at different distances from the RNA. At one extreme are chelated cations, in which direct contacts with the RNA have displaced some of the first hydration layer of the ion. Chelated $K^+$ and $Mg^{2+}$ are both found in RNA crystal structures; in one instance, these two ions are buried side-by-side within a ribosomal RNA fragment (Fig. 1 *A*). Only a small fraction of the total RNA charge is ever neutralized by chelated cations. Only ~60 chelated $Mg^{2+}$ have been identified among the ~3000 nucleotides of the large subunit ribosome (8), and most high-resolution RNA crystal structures do not show any chelated ions at all. At the other extreme, ''diffuse'' ions remain largely hydrated and only interact with the electrostatic potential that extends many ångstroms from the RNA surface. Fig. 1 *B* illustrates the intensity of the RNA electrostatic potential (red shading) and the corresponding concentration gradient of diffuse cations (contour lines) around an RNA, the so-called ''ion atmosphere''. Between the extremes of diffuse and chelated ions, ions may interact with the RNA surface indirectly via hydrogen-bonding between the first ion

*Submitted July 26, 2008, and accepted for publication September 12, 2008.*

Address reprint requests to David E. Draper, Dept. of Chemistry, The Johns Hopkins University, Baltimore, MD 21218. Tel.: 410-516-7448; Fax: 410-516-8420; E-mail: draper@jhu.edu.

Editor: Edward H. Egelman.


0006-3495/08/12/5489/07 $2.00

doi: 10.1529/biophysj.108.131813

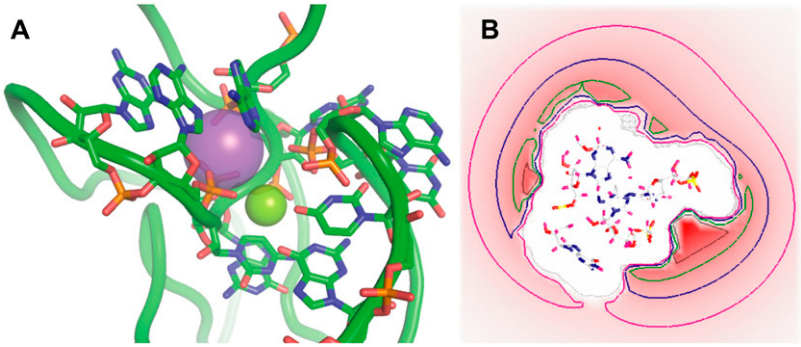


FIGURE 1 Ions in and near RNAs. (*A*) Chelated ions in an rRNA fragment (PDB file 1hc8 (30)). $K^+$ (*violet*) and $Mg^{2+}$ (*light green*) ions are shown as translucent spheres sized according to their Pauling ionic radii (1.33 and 0.65 Å, respectively). Nucleotides having atoms within 5.0 Å of either ion are drawn; only the backbone is shown for the remainder of the RNA. (*B*) Calculated electrostatic potential around a cross section of an RNA hairpin; the darkest red shading corresponds to −3 kT/e and white is zero potential. Contour lines illustrate the cation gradient, corresponding to concentrations of 0.2, 0.4, 0.8, and 1.6 M. The bulk salt concentration at zero potential is 0.1 M (adapted from García-García and Draper (26)).

hydration layer and RNA acceptors. Lastly, anions are depleted near the RNA because of electrostatic repulsion.

A comprehensive analysis of ion-RNA energetics is exceedingly difficult, because of the variety of possible ion environments and the different interaction energies that dominate in each environment. Coulombic and hydration energies are usually the largest, but ion polarization and other factors may be important in some contexts (9). In addition, it is not possible to break down the problem into classes of independently behaving classes of ions; the long-range nature of coulombic forces creates strong thermodynamic linkage between all ions interacting with an RNA (10). However, theoretical developments and quantitative experiments over the last decade have succeeded in clarifying some aspects of the problem. The following sections first present a purely thermodynamic formalism for describing mono- and divalent ion-RNA interactions, and then move to a molecular interpretation of these interactions and remarks on the computational and experimental challenges that remain.

## Energetics of monovalent ion-RNA interactions

A purely thermodynamic description of the interactions between ions and a polynucleotide begins with the so-called interaction coefficients, defined for monovalent cations as

$$\Gamma_+ \equiv \left(\frac{\partial m_+}{\partial m_{PN}}\right)_{\mu_+} \approx \left(\frac{m_+ - m_{bulk}}{m_{PN}}\right)_{\mu_+}, \qquad (1)$$

where $m_+$ and $m_{PN}$ are the molalities of the monovalent cation and polynucleotide, respectively. $\Gamma_+$ can be measured in an equilibrium dialysis experiment by comparing the cation concentration present in solution with the RNA ($m_+$) with the ''bulk'' concentration present on the other side of the dialysis membrane ($m_{bulk}$). $\Gamma_+$ thus represents the ''excess'' number of cations accumulated by an RNA due to all interactions, including chelation and the concentration gradient of diffuse ions (Fig. 1, *A* and *B*). The chemical potential of the cations, $\mu_+$, must be the same on both sides of the membrane at equilibrium; thus the higher concentration of the cations in the RNA solution requires their activity coefficient to be less than that of the bulk ions (see Eqs. 15 and 16 of Record et al. (11)). The decreased activity is related to the favorable free energy of cation-RNA interaction. An analogous quantity, $\Gamma_-$, measures the anion deficit ($m_- - m_{bulk}$ is negative) in dialysis equilibrium with the polynucleotide; anion activity coefficients increase in the presence of RNA because of unfavorable interactions. $\Gamma_+$ and $|\Gamma_-|$ also represent the number of polynucleotide phosphate charges that are neutralized by the excess of cations or by the deficiency of anions, respectively, and together must add to the total negative charge of the RNA.

Strauss et al. (12) used equilibrium dialysis to measure $\Gamma_-$ for double helical DNA over a wide range of salt concentrations, and similar measurements have been extended recently to DNA oligomers (13). In both cases, $\Gamma_+$ is much larger than $|\Gamma_-|$ at low to moderate salt concentrations. This preference for neutralizing the DNA charge by cation excess is the hallmark of the ''polyelectrolyte effect'' (14). It is attributable to the very negative electrostatic potential of a high charge density polynucleotide; accumulation of a high concentration of nearby cations much more effectively reduces the electrostatic free energy than does exclusion of anions, which (at lower salt concentrations) are relatively dilute compared to the local concentration of phosphates. An important principle is that $\Gamma_+$ increases (and $\Gamma_-$ becomes less negative) with increasing charge density of a polynucleotide. Thus both $\Gamma_+$ and $\Gamma_-$ increase in the transition from single-stranded to helical DNA, and by LeChatelier's principle, added salt stabilizes the higher charge density helical form (15).

The polyelectrolyte effect also applies to irregular RNA structures. RNAs generally become more compact and develop higher charge density in the series $U \rightarrow I \rightarrow N$; added monovalent salt thus favor the native form. But the sensitivity of RNA tertiary structures to salt differs in two important ways from the response of helical DNA. First, calculations (10,16,17) and experiment (18) suggest that RNA tertiary structures may develop much more negative electrostatic potentials than a DNA helix. The more negative electrostatic potential increases the concentration of diffuse cations close to the RNA surface, where ion properties besides charge (e.g., radius, hydration energy) may become consequential. Second, monovalent ions may be chelated by irregular RNA

structures (Fig. 1 *A*). Both of these factors may make the stability of an RNA tertiary structure sensitive to the size of the monovalent cation that is present (19,20), in contrast to the weak discrimination shown by DNA helices in their interactions with different group I ions (13,19).

## Energetics of divalent cation-RNA interactions

A striking feature of RNA sensitivity to ions is the very large stabilizing influence of $Mg^{2+}$ on RNA tertiary structure, even in the presence of more than a 100-fold excess of monovalent cations (3). Much of the older RNA folding literature discussed this phenomenon in terms of a simplified model originally derived in reference to cooperative binding of uncharged ligands to fixed sites on proteins (21). This approach did not take into account the high charge densities and long-range electrostatic interactions that heavily influence ion-RNA interactions. Because of these deficiencies, this early model presupposed an essential role for a small number of $Mg^{2+}$ ions binding at chelated sites in the native structure, and implicitly assuming that the interactions of diffuse ions with both the partially unfolded *I* state and the *N* state are insignificant.

An alternative approach for evaluating $Mg^{2+}$-RNA interactions is the formalism described in the preceding section (Eq. 1), which is easily extended to include an interaction coefficient for the excess $Mg^{2+}$ ion, $\Gamma_{2+}$, in addition to the terms for monovalent ions, $\Gamma_+$ and $\Gamma_-$ (22). Analogous to the case of monovalent cations, the total free energy of all $Mg^{2+}$-RNA interactions is reflected by a decrease in the $Mg^{2+}$ activity coefficient in the presence of RNA and by a positive value of $\Gamma_{2+}$. Using this formalism to analyze appropriate titration experiments, the overall free energy of $Mg^{2+}$-RNA interactions can be measured without any prior assumptions about the types of environments occupied by the ions (23). (Note that $\Gamma_{2+}$ can only be measured in the presence of an excess of monovalent salt large enough to insure that neither the total $Cl^-$ concentration nor the $Mg^{2+}$ activity coefficient change significantly during a titration with $MgCl_2$.)

$\Gamma_{2+}$ has been measured for a pseudoknot RNA in its native tertiary fold (*N* state) and for a sequence variant trapped in a partially unfolded form that mimics the *I* state of the same RNA (Fig. 2 *A*, *upper panel*) (24). (Instead of measuring $\Gamma_{2+}$ by equilibrium dialysis, a fluorescent dye monitored $Mg^{2+}$ activity in the presence of RNA (23).) Integration under these titration curves gives the overall free energies of $Mg^{2+}$ interactions, $\Delta G_{I-2+}$ and $\Delta G_{N-2+}$ (Fig. 2 *A*, *lower panel*). It is clear that $Mg^{2+}$ interactions with the *I* state cannot be ignored: on folding to the *N* state, there is only a small increment in either the number of excess $Mg^{2+}$ ions or their overall free energy of interaction with the RNA.

The pseudoknot RNA readily folds into its native structure in the presence of moderate concentrations of monovalent ions alone. In contrast, even molar concentrations of KCl do not induce folding of a 58mer rRNA fragment in the absence of $Mg^{2+}$ (18). An *I* state mimic of this RNA interacts with $Mg^{2+}$ much more strongly than does helical DNA (Fig. 2 *B*), presumably because the three-helix junction present in the *I* state has a higher charge density than a regular helix. When the native sequence of this RNA is titrated with $Mg^{2+}$, the transition to the folded state coincides with an inflection in the $\Gamma_{2+}$ curve (Fig. 2 *B*, *arrow*). Because of the folding transition taking place, $\Delta G_{N-2+}$ cannot be determined by integration of these titration data, but rough estimation of $\Delta G_{N-2+}$ by other means suggests that it is ~6-fold more negative than $\Delta G_{I-2+}$ (23). The two RNAs shown in Fig. 2 thus present interesting extremes in the degree to which an $I \rightarrow N$ folding transition enhances RNA interactions with $Mg^{2+}$. The challenge, of course, is to understand these behaviors at a detailed molecular level.

## Molecular interpretations of cation-RNA interaction energetics

### *Theoretical descriptions of the ion atmosphere*

Thermodynamic descriptions of ion-RNA interactions, as embodied in interaction coefficients and free energies, do not show the spatial distribution of ions near an RNA or inform

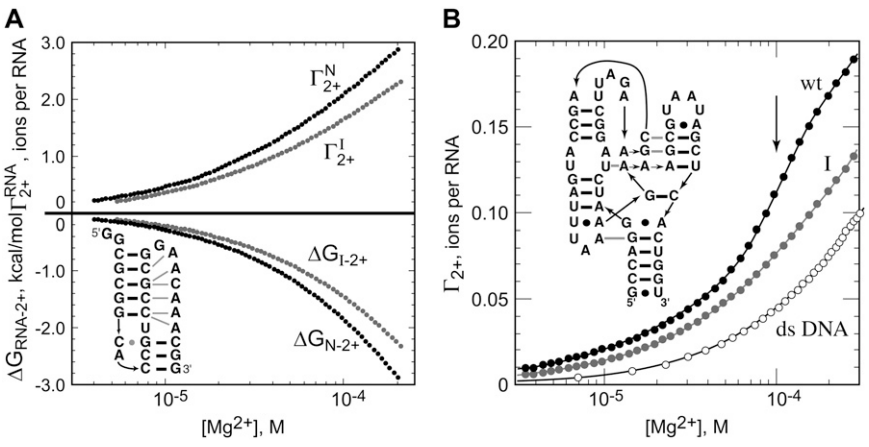


FIGURE 2 $Mg^{2+}$ interactions with two RNAs. Diagrams of the RNA secondary (*black bars*) and tertiary (*gray bars*) base-base hydrogen bonding are shown as insets. (*A*) $\Delta G_{RNA-2+}$ (*lower panel*) and $\Gamma_{2+}$ (*upper panel*) measured for a folded pseudoknot (*N*, *dark symbols*) and a mutant sequence unable to fold (*I*, *gray symbols*), in the presence of 54 mM $K^+$ (24). (*B*) $\Gamma_{2+}$ measured for a 58 nucleotide rRNA fragment (wt, *black solid circles*) and for a mutant RNA unable to fold tertiary structure (*I*, *gray solid circles*). The midpoint of the RNA folding transition to its native structure occurs at 0.1 mM $Mg^{2+}$ (*arrow*) under the conditions used in these measurements (60 mM $K^+$, 15°C) (23). For comparison, $\Gamma_{2+}$ for double stranded DNA (also in buffer with 60 mM $K^+$) is shown (*open circles*).

as to the kinds of environments occupied by the ions. Molecular interpretations of the measurements must rely on theoretical models that attempt to quantitatively account for $\Gamma_{ion}$ and the corresponding interaction free energies. The most widely used models have been based on Poisson-Boltzmann (PB) theories, which consider cation accumulation and anion depletion as Boltzmann-weighted distributions of ions according to the mean electrostatic potential of the RNA. Among the simplifications made in PB theories, neither water molecules nor ions are discrete and no provision is made for ion hydration energies to vary with ion position relative to the RNA. PB-based models are therefore expected to perform best when the free energy of ion-RNA interaction is dominated by diffuse ions, and may become problematic as higher concentrations of ions accumulate close to the RNA surface. With regard to monovalent ions, a cylindrical PB model successfully accounts for the salt dependences of duplex and triplex RNA and DNA unfolding transitions (15); the nonlinear PB equation (NLPBe) provides a good description of the distribution of ions around a DNA as detected in x-ray scattering experiments (25) and quantitatively describes the influence of the monovalent ion atmosphere on the binding of basic peptides to an RNA hairpin (26). PB-based theories have recently been modified to take explicit account of ion size, by introduction of a term for ion excluded volume into NLPBe (13) and by a hybrid model with explicit ions near the nucleic acid surface and a continuum model further away (27).

Divalent cations interactions with RNA are stronger than those of monovalent ions, and the NLPBe underestimates experimental measurements of $\Gamma_{2+}$ and $-\Delta G_{RNA-2+}$ for folded (*N* state) and partially unfolded (*I* state) forms of the RNA pseudoknot in Fig. 2 *A* by ~30% (24). Because the underestimation is similar for the two forms, the calculated *differences* between *N* and *I* state values of $\Gamma_{2+}$ and $\Delta G_{RNA-2+}$ are in good agreement with the experimental data (23,24). Similar agreement is found between calculated and experimental stabilization of tRNA by $Mg^{2+}$ (28). These two RNAs do not have chelated ions, and the results are consistent with most of the energetic contribution of $Mg^{2+}$ to RNA stabilization coming from the stronger interactions of diffuse ions with the higher charge density of the native RNA.

Calculations with the NLPBe provide a simple insight as to why diffuse $Mg^{2+}$ ions are so much more effective than monovalent ions in stabilizing compact RNA structures. In folding tertiary structure, the charge density and negative electrostatic potential of an RNA increase dramatically, cations are pulled closer to the RNA surface, and there is an unfavorable decrease in their translational entropy. But this entropic penalty is smaller for $Mg^{2+}$ than for monovalent ions, simply because half as many excess divalent ions are needed to neutralize the same negative charge. The net ion-RNA electrostatic free energy is slightly more favorable when one $Mg^{2+}$ is replaces two excess $K^+$, but it is mainly the inherent entropic advantage of the exchange that accounts for the large stabilizing influence of diffuse $Mg^{2+}$ (28). A corollary of this analysis is that trivalent ions should be even more stabilizing than $Mg^{2+}$, which is consistent with experiment (29). Note that this entropic effect is expected to contribute a substantial stabilization free energy to all RNA tertiary structures, even those with tightly chelated $Mg^{2+}$ (see below).

### *Free energies of ion chelation*

There have been a few attempts to calculate the free energy of placing $K^+$ or $Mg^{2+}$ at a specific RNA chelation site (9,10,30). At a minimum, several large free energies must be estimated: the penalties for dehydrating the ion and RNA binding site, the surprisingly large repulsive energy between the bound ion and the ion atmosphere, and the favorable interaction of the ion with the electrostatic potential of the chelation site. Chelation sites tend to be pockets that are partially or fully buried within the RNA structure and lined with electronegative oxygen, and as such may develop extraordinarily negative electrostatic potentials that more than compensate for the costs of ion dehydration and ion atmosphere repulsion. In some cases, a single $Mg^{2+}$ chelation site may contribute a large fraction of the total stabilization from all the $Mg^{2+}$ ions interacting with an RNA (10).

Although a chelated $Mg^{2+}$ may be very stabilizing, formation of a chelation site comes at the high cost of burying electronegative oxygen in the interior of an RNA. In the case of the RNA shown in Fig. 1 *A*, the folding free energy in the absence of $Mg^{2+}$ is estimated as a highly unfavorable +19 kcal/mol (23) and the net stability under physiological salt conditions is not much different than that of a pseudoknot lacking chelated ions (Fig. 2 *A*). From this perspective, chelated ions confer no particular advantage in terms of RNA stability, but they do increase the variety of folding strategies available to an RNA. To create ligand binding sites or ribozyme active sites, it may be difficult to avoid a folding topology that protects some of the RNA backbone from solvent. Such intrinsically unstable architectures become energetically feasible only if the protected phosphates are neutralized by chelated ions.

The distinction between diffuse and chelated ions has been a useful framework for developing quantitative theoretical accounts of overall $Mg^{2+}$-RNA interaction free energies. A more sophisticated framework will undoubtedly be needed to describe the ions and water in close proximity to the RNA, especially at the level of accuracy required to understand the roles of ions in ribozyme mechanisms, in stabilization of codon-anticodon interactions in the ribosome, or in other RNA functional centers where solvent access is restricted.

## Characterization of the *I* state

The *I* state of an RNA is an ensemble of structures, which potentially include alternative secondary structures and cer-

tainly differ in the detailed arrangement of helical segments in space. Neutron and x-ray scattering experiments have been used by several groups to define the average extension of partially unfolded RNA (18,31–34), and in some instances the scattering curve has been used to deduce the average shape of a partially unfolded RNA (35). Resonance energy transfer between fluorescent tags, attached to specific positions within an RNA, has the potential to resolve the distribution of distances among *I* state conformers, particularly when single molecule observations are made. Such experiments have suggested that the *I* state sometimes consists of distinct, coexisting subpopulations (36–38). Other kinds of experiments have supported the existence of distinct *I* states with partially formed tertiary structure (33,34).

In the scattering studies just cited, the degree to which an RNA *I* state is extended or compacted depends on the concentrations of mono- and divalent cations that are present. The most highly extended structures seen at very low monovalent salt concentrations (<10 mM) may reflect ''fraying'' at the ends of helical segments. But at higher salt concentrations, compaction certainly benefits from the reduced electrostatic repulsion between phosphate charges, in the same way that salt reduces the radius of gyration of linear charged polymers (39). $Mg^{2+}$ is far more effective than monovalent cations in promoting compact conformations, consistent with the entropic advantage of $Mg^{2+}$ over monovalent ions in stabilizing compact structures (noted above), and most models of large RNA folding pathways include a $Mg^{2+}$-induced ''collapse'' of the *I* state preceding formation of tertiary structure (40–42). An interesting notion is that $Mg^{2+}$ might not just reduce phosphate repulsion, but induce an attractive force between helical segments in a large RNA, either because of fluctuating dipoles caused by ion correlation (29) or because of an entropic advantage in merging ion atmospheres (43). Theoretical considerations have long suggested the existence of such an attractive force ((44), and references therein). But to date, scattering measurements have failed to detect $Mg^{2+}$-induced attraction between helical DNA oligomers, except at high $Mg^{2+}$ concentrations with minimal monovalent ion present, far outside physiological ranges of ion concentrations (45,46).

## Sensitivity of RNA folding to $Mg^{2+}$

In a common experiment, the extent of RNA folding to its native state is followed as $MgCl_2$ is titrated (Fig. 3 *A*), from which an observed free energy of folding ($\Delta G^\circ_{obs,2+} = -RT ln([N]/[I])$) is calculated as a function of $Mg^{2+}$ concentration. A thermodynamic cycle summarizes the balance of free energies that determine the shape of the curve (Fig. 3 *B*). The RNA has an intrinsic $\Delta G^\circ$ of folding in the absence of $Mg^{2+}$ ($\Delta G^\circ_{obs,0}$), which is frequently unfavorable, but a net stabilizing free energy is provided by the difference in $Mg^{2+}$ interaction free energies with *N* and *I* state conformations: $\Delta G^\circ_{obs,2+} = \Delta G^\circ_{obs,0} + (\Delta G_{N-2+} - \Delta G_{I-2+})$. Mutations that disrupt tertiary structure generally shift the midpoint of such titration curves to a higher $Mg^{2+}$ concentration (47). Because a mutation may affect any of the three free energy terms comprising $\Delta G^\circ_{obs,0}$, the magnitude of the shift does not give further insight into the way the mutation affects RNA interactions with $Mg^{2+}$, unless other free energies of the cycle can be measured independently. But for the important class of RNAs that only fold in the presence of $Mg^{2+}$, it is difficult to estimate $\Delta G^\circ_{obs,0}$ and $\Delta G_{N-2+}$ cannot be measured directly (Fig. 2 *B*). There is consequently a lack of experimental information about the magnitude and origins of the stabilizing effects of $Mg^{2+}$ for many RNAs, which is a serious limitation in testing quantitative model of $Mg^{2+}$-RNA interactions.

An informative aspect of these $Mg^{2+}$ titration curves is the slope at the midpoint, which can be very steep or shallow depending on the specific RNA. A thermodynamic linkage

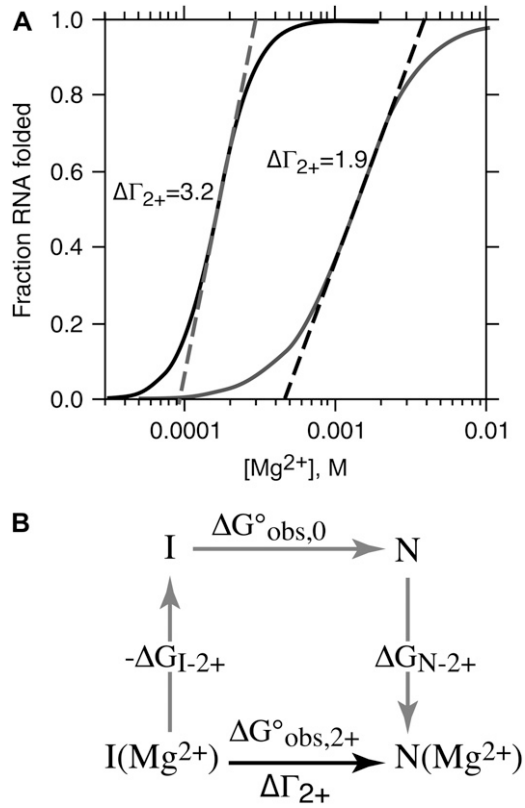


FIGURE 3 Sensitivity of RNA folding to $Mg^{2+}$ concentration. (*A*) Calculated dependence of the fraction of RNA folded on $Mg^{2+}$ concentration. $\Delta G_{I-2+}$ and $\Delta G_{N-2+}$ were derived from NLPB-based calculations for a 58 nt rRNA fragment in 60 mM monovalent salt, using the crystal structure for the *N* state or models of the *I* state as described (18). $\Delta G^\circ_{obs,0}$ was arbitrarily set to 6 kcal/mol. Transitions from an extended *I* state ($R_g$ = 25 Å, *black curve*) or a compact *I* state ($R_g$ = 20 Å, *gray curve*) to the *N* state are shown. Values of $\Delta\Gamma_{2+}$ for each curve have been calculated for the midpoint of the titration curve. (*B*) A thermodynamic cycle accounting for the effect of $Mg^{2+}$ on an RNA folding transition. The measured free energy of folding at a particular set of monovalent and divalent ion concentrations, $\Delta G^\circ_{obs,2+}$, is the sum of the intrinsic free energy of folding in the absence of $Mg^{2+}$ ($\Delta G^\circ_{obs,0}$) and the free energies of $Mg^{2+}$ interaction with either *I* or *N* states of the RNA ($\Delta G_{I-2+}$, $\Delta G_{N-2+}$).

equation relates the slope at the midpoint of the titration curve to $\Delta\Gamma_{2+}$, the increase in excess ions that is associated with the folding reaction (22). Because the major determinant of the magnitude of $\Gamma_{2+}$ is the charge density of the RNA, $\Delta\Gamma_{2+}$ is largely a measure of the degree of compaction that an RNA undergoes on folding (A common misconception is that $\Delta\Gamma_{2+}$ is related to the number of chelation sites created when an RNA folds. In ranges of $Mg^{2+}$ and $K^+$ concentration near physiological, $\Gamma_{2+}$ is relatively sensitive too the presence of chelated ions: if a $Mg^{2+}$ ion becomes bound at a specific site, the excess $Mg^{2+}$ associated with the ion atmosphere is reduced by a nearly compensating number (18). Thus, $\Gamma_{2+}$ is generally more sensitive to charge density than to the specific environments occupied by the ions.) To illustrate this point, the NLPBe was used to calculate $\Gamma_{2+}$ for two *I* state models of a 58 nt rRNA fragment, with radii of gyration ($R_g$) of 25 or 20 Å (18). When combined with calculations of $\Gamma_{2+}$ based on the crystal structure of the native RNA ($R_g = 16.9$ Å), the resulting $Mg^{2+}$ titration curves show that folding from the more extended *I* state conformation produces a considerably steeper dependence on $Mg^{2+}$ concentration (Fig. 3 *A*).

An mRNA conformational switch that controls expression of $Mg^{2+}$ transporter genes (48) illustrates how the magnitude of $\Delta\Gamma_{2+}$ can be functionally important. This riboswitch folds in response to a small, 2–3-fold increment in $Mg^{2+}$ concentration; presumably the smaller this increment, the more precisely intracellular $Mg^{2+}$ levels can be controlled. According to the ideas developed in this review, selective pressure for a large $\Delta\Gamma_{2+}$ would favor a relatively large RNA undergoing a transition from an extended *I* state to a compact N state. The switch structure in fact is large (185 nt), undergoes a large change in sedimentation coefficient on folding, and adopts a very compact structure in the native form (48). Other riboswitches that sense small organic metabolites are also stabilized by $Mg^{2+}$, but respond over a 100-fold range of $Mg^{2+}$ concentrations (35,49). These RNAs are presumably selected to be insensitive to small fluctuations in the intracellular $Mg^{2+}$ activity.

## CONCLUSION

This review has pointed out several simple concepts that underlie much of the response of an RNA to changes in ion concentration: the increases in $\Gamma_{ion}$ that accompany the folding of an RNA to a more compact and higher charge density structure; the entropic advantage of accumulating divalent ions in the ion atmosphere of high charge density RNAs; and the need to compensate the charge of solvent-inaccessible backbone by chelated ions. Progress has been made in developing quantitative pictures of all of these aspects of RNA folding, but clearly much more work remains to be done. More detailed experimental insights are needed as to the nature of the ion atmosphere, the ensemble of *I* state structures, and the energetics of ion-RNA interactions. Likewise, more sophisticated theoretical approaches, especially ones whose results can be compared with experimental benchmarks, would help interpret experimental results. The relevance of ion interactions to the function of RNA in the cellular economy should continue to motivate studies in this field.

This work was supported by the National Institutes of Health grant No. GM58545.

## REFERENCES

1. Cate, J. H., A. R. Gooding, E. Podell, K. Zhou, B. L. Golden, C. E. Kundrot, T. R. Cech, and J. A. Doudna. 1996. Crystal structure of a group I ribozyme domain: principles of RNA packing. *Science*. 273: 1678–1685.
2. Cole, P. E., S. K. Yang, and D. M. Crothers. 1972. Conformational changes of transfer ribonucleic acid. equilibrium phase diagrams. *Biochemistry*. 11:4358–4368.
3. Stein, A., and D. M. Crothers. 1976. Conformational changes of transfer RNA. The role of magnesium(II). *Biochemistry*. 15:160–167.
4. Breaker, R. R. 2008. Complex riboswitches. *Science*. 319:1795–1797.
5. Cayley, S., B. A. Lewis, H. J. Guttman, and M. T. Record Jr. 1991. Characterization of the cytoplasm of *Escherichia coli* K-12 as a function of external osmolarity. Implications for protein-DNA interactions in vivo. *J. Mol. Biol.* 222:281–300.
6. Froschauer, E. M., M. Kolisek, F. Dieterich, M. Schweigel, and R. J. Schweyen. 2004. Fluorescence measurements of free [$Mg^{2+}$] by use of mag-fura 2 in *Salmonella enterica*. *FEMS Microbiol. Lett.* 237:49–55.
7. London, R. E. 1991. Methods for measurement of intracellular magnesium: NMR and fluorescence. *Annu. Rev. Physiol.* 53:241–258.
8. Klein, D. J., P. B. Moore, and T. A. Steitz. 2004. The contribution of metal ions to the structural stability of the large ribosomal subunit. *RNA*. 10:1366–1379.
9. Petrov, A. S., G. Lamm, and G. R. Pack. 2005. Calculation of the binding free energy for magnesium-RNA interactions. *Biopolymers*. 77:137–154.
10. Misra, V. K., and D. E. Draper. 2001. A thermodynamic framework for $Mg^{2+}$ binding to RNA. *Proc. Natl. Acad. Sci. USA*. 98:12456–12461.
11. Record, M. T., Jr., W. Zhang, and C. F. Anderson. 1998. Analysis of effects of salts and uncharged solutes on protein and nucleic acid equilibria and processes: a practical guide to recognizing and interpreting polyelectrolyte effects, Hofmeister effects, and osmotic effects of salts. *Adv. Protein Chem.* 51:281–353.
12. Strauss, U. P., C. Helfgott, and H. Pink. 1967. Interactions of polyelectrolytes with simple electrolytes. II. Donnan equilibria obtained with DNA in solutions of 1–1 electrolytes. *J. Phys. Chem.* 71: 2550–2556.
13. Bai, Y., M. Greenfeld, K. J. Travers, V. B. Chu, J. Lipfert, S. Doniach, and D. Herschlag. 2007. Quantitative and comprehensive decomposition of the ion atmosphere around nucleic acids. *J. Am. Chem. Soc.* 129:14981–14988.
14. Anderson, C. F., and M. T. Record Jr. 1993. Salt dependence of oligoion-polyion binding: a thermodynamic description based on preferential interaction coefficients. *J. Phys. Chem.* 97:7116–7126.
15. Bond, J. P., C. F. Anderson, and M. T. Record Jr. 1994. Conformational transitions of duplex and triplex nucleic acid helices: thermodynamic analysis of effects of salt concentration on stability using preferential interaction coefficients. *Biophys. J.* 67:825–836.
16. Chin, K., K. A. Sharp, B. Honig, and A. M. Pyle. 1999. Calculating the electrostatic properties of RNA provides new insights into molecular interactions and function. *Nat. Struct. Biol.* 6:1055–1061.
17. Misra, V. K., and D. E. Draper. 2000. $Mg(^{2+})$ binding to tRNA revisited: the nonlinear Poisson-Boltzmann model. *J. Mol. Biol.* 299: 813–825.

18. Grilley, D., V. Misra, G. Caliskan, and D. E. Draper. 2007. Importance of partially unfolded conformations for $Mg(^{2+})$-induced folding of RNA tertiary structure: structural models and free energies of $Mg(^{2+})$ interactions. *Biochemistry*. 46:10266–10278.
19. Shiman, R., and D. E. Draper. 2000. Stabilization of RNA tertiary structure by monovalent cations. *J. Mol. Biol.* 302:79–91.
20. Heerschap, A., J. A. L. I. Walters, and C. W. Hilbers. 1985. Interactions of some naturally occurring cations with phenylalanine and initiator tRNA from yeast as reflected by their thermal stability. *Biophys. Chem.* 22:205–217.
21. Schimmel, P. R., and A. G. Redfield. 1980. Transfer RNA in solution: selected topics. *Annu. Rev. Biophys. Bioeng.* 9:181–221.
22. Grilley, D., A. M. Soto, and D. E. Draper. 2006. Direct quantitation of $Mg^{2+}$-RNA interactions by use of a fluorescent dye. *Methods Enzymol.* In press.
23. Grilley, D., A. M. Soto, and D. E. Draper. 2006. $Mg^{2+}$-RNA interaction free energies and their relationship to the folding of RNA tertiary structures. *Proc. Natl. Acad. Sci. USA.* 103:14003–14008.
24. Soto, A. M., V. Misra, and D. E. Draper. 2007. Tertiary structure of an RNA pseudoknot is stabilized by ''diffuse'' Mg(2+) ions. *Biochemistry.* 46:2973–2983.
25. Das, R., T. T. Mills, L. W. Kwok, G. S. Maskel, I. S. Millett, S. Doniach, K. D. Finkelstein, D. Herschlag, and L. Pollack. 2003. Counterion distribution around DNA probed by solution x-ray scattering. *Phys. Rev. Lett.* 90:188103.
26. García-García, C., and D. E. Draper. 2003. Electrostatic interactions in a peptide-RNA complex. *J. Mol. Biol.* 331:75–88.
27. Tan, Z. J., and S. J. Chen. 2006. Nucleic acid helix stability: effects of salt concentration, cation valence and size, and chain length. *Biophys. J.* 90:1175–1190.
28. Misra, V. K., and D. E. Draper. 2002. The linkage between magnesium binding and RNA folding. *J. Mol. Biol.* 317:507–521.
29. Heilman-Miller, S. L., D. Thirumalai, and S. A. Woodson. 2001. Role of counterion condensation in folding of the Tetrahymena ribozyme. I. Equilibrium stabilization by cations. *J. Mol. Biol.* 306:1157–1166.
30. Conn, G. L., A. G. Gittis, E. E. Lattman, V. K. Misra, and D. E. Draper. 2002. A compact RNA tertiary structure contains a buried backbone-$K^+$ complex. *J. Mol. Biol.* 318:963–973.
31. Perez-Salas, U. A., P. Rangan, S. Krueger, R. M. Briber, D. Thirumalai, and S. A. Woodson. 2004. Compaction of a bacterial group I ribozyme coincides with the assembly of core helices. *Biochemistry.* 43:1746–1753.
32. Takamoto, K., R. Das, Q. He, S. Doniach, M. Brenowitz, D. Herschlag, and M. R. Chance. 2004. Principles of RNA compaction: insights from the equilibrium folding pathway of the P4–P6 RNA domain in monovalent cations. *J. Mol. Biol.* 343:1195–1206.
33. Chauhan, S., G. Caliskan, R. M. Briber, U. Perez-Salas, P. Rangan, D. Thirumalai, and S. A. Woodson. 2005. RNA tertiary interactions mediate native collapse of a bacterial group I ribozyme. *J. Mol. Biol.* 353:1199–1209.
34. Baird, N. J., E. Westhof, H. Qin, T. Pan, and T. R. Sosnick. 2005. Structure of a folding intermediate reveals the interplay between core and peripheral elements in RNA folding. *J. Mol. Biol.* 352:712–722.
35. Lipfert, J., R. Das, V. B. Chu, M. Kudaravalli, N. Boyd, D. Herschlag, and S. Doniach. 2007. Structural transitions and thermodynamics of a glycine-dependent riboswitch from *Vibrio cholerae*. *J. Mol. Biol.* 365: 1393–1406.
36. Pljevaljcic, G., D. P. Millar, and A. A. Deniz. 2004. Freely diffusing single hairpin ribozymes provide insights into the role of secondary structure and partially folded states in RNA folding. *Biophys. J.* 87:457–467.
37. Xie, Z., N. Srividya, T. R. Sosnick, T. Pan, and N. F. Scherer. 2004. Single-molecule studies highlight conformational heterogeneity in the early folding steps of a large ribozyme. *Proc. Natl. Acad. Sci. USA.* 101:534–539.
38. Lemay, J. F., J. C. Penedo, R. Tremblay, D. M. Lilley, and D. A. Lafontaine. 2006. Folding of the adenine riboswitch. *Chem. Biol.* 13: 857–868.
39. Schneider, N. S., and P. Doty. 1954. Macro-Ions IV. The ionic strength dependence of the molecular properties of sodium carboxymethylcellulose. *J. Phys. Chem.* 58:762–769.
40. Sclavi, B., M. Sullivan, M. R. Chance, M. Brenowitz, and S. A. Woodson. 1998. RNA folding at millisecond intervals by synchrotron hydroxyl radical footprinting. *Science.* 279:1940–1943.
41. Buchmueller, K. L., A. E. Webb, D. A. Richardson, and K. M. Weeks. 2000. A collapsed non-native RNA folding state. *Nat. Struct. Biol.* 7:362–366.
42. Russell, R., I. S. Millett, S. Doniach, and D. Herschlag. 2000. Small angle x-ray scattering reveals a compact intermediate in RNA folding. *Nat. Struct. Biol.* 7:367–370.
43. Murthy, V. L., and G. D. Rose. 2000. Is counterion delocalization responsible for collapse in RNA folding? *Biochemistry.* 39:14365–14370.
44. Tan, Z. J., and S. J. Chen. 2006. Ion-mediated nucleic acid helix-helix interactions. *Biophys. J.* 91:518–536.
45. Bai, Y., R. Das, I. S. Millett, D. Herschlag, and S. Doniach. 2005. Probing counterion modulated repulsion and attraction between nucleic acid duplexes in solution. *Proc. Natl. Acad. Sci. USA.* 102:1035–1040.
46. Qiu, X., K. Andresen, L. W. Kwok, J. S. Lamb, H. Y. Park, and L. Pollack. 2007. Inter-DNA attraction mediated by divalent counterions. *Phys. Rev. Lett.* 99:038104.
47. Silverman, S. K., and T. R. Cech. 1999. Energetics and cooperativity of tertiary hydrogen bonds in RNA structure. *Biochemistry.* 38:8691–8702.
48. Dann 3rd, C. E., C. A. Wakeman, C. L. Sieling, S. C. Baker, I. Irnov, and W. C. Winkler. 2007. Structure and mechanism of a metal-sensing regulatory RNA. *Cell.* 130:878–892.
49. Hampel, K. J., and M. M. Tinsley. 2006. Evidence for preorganization of the glmS ribozyme ligand binding pocket. *Biochemistry.* 45:7861–7871.